

Validity of modified charge transport model of organic polymers for electron only and hole only devices

MUHAMMAD AMMAR KHAN*

Department of Physical and Numerical Sciences, Qurtuba university of Science and Information Technology, D. I. Khan, Pakistan

Charge transport models are rapidly developing research area in the field of organic semiconductor devices. In this work organic materials have been theoretically studied and focusing on the electrical characteristic of organic polymers. On the basis of the modification of improved Current Density-Voltage formula-based charge transport model is applied to different hole only and electron only devices of various thickness at different temperature. By considering organic semiconductors are nondegenerate and solving the drift-diffusion equation, the mobility with respect to temperature and current-voltage data for all materials (fluctuation between theoretical curves and experimental data points) are good fitted. Taking into consideration of electric field dependence of mobility this research work gives good reasonable results with suitable parameters. This work also support the quantum chemical study that for polymer, poly{[N,N'-bis(2-octyldodecyl)naphthalene-1,4,5,8-bis(dicarboximide)-2,6-diyl]-alt-5,5'-(2,2'-dithiophene)} [P(NDI2OD-T2),N2200], the electron mobility is observed to be more than the hole mobility. As compare to previous transport models this improved formula-based transport model is accurate because determination of results from the modified transport model are in good agreement with the complete numerical solutions. This work verifies that this formula-based charge transport model covers a large number of semiconducting materials and helps to modify the semiconductor devices in more precise form with better performance.

(Received December 21, 2022; accepted June 9, 2023)

Keywords: Charge transport, Organic diode, Non-symmetric potential barriers, Polymers, New density of states (DOS)

1. Introduction

The study of organic semiconductors has become hot topics in recent years due to their merits that less expensive, very easy to fabricate, and many potential applications, such as; organic solar cells, organic semiconductor lasers, organic thermoelectric devices, organic light emitting diodes (OLEDs), organic detectors and sensors and, and flexible electronics devices [1]. Nowadays there is hardly any device without the existence of semiconductor.

If the organic semiconductor material can be used in the active layer of the electronic component, it can be a plastic with a higher degree of flexibility as the substrate of electronic components. Organic semiconductors can be manufactured at room temperature, and their production is much easier and cheaper than for conventional silicon and inorganic semiconductors. Organic semiconductor research has brought new vitality in organic semiconductor technology. Organic semiconductor materials have 50 years of history [2]. In this short period, organic semiconductor materials research raised from simple basic to the practical stage. On the basis of this research many of organic semiconductor devices invented. Scientist are trying to find the new organic material and their usage in electronic devices. A lot of researchers have a contribution in the field of electronics theoretically and experimentally and accelerated the organic semiconductor field [3-5].

Organic semiconductor can overcome a lot of shortcoming in inorganic semiconductors. This was the major breakthrough in the field of organic semiconductor, when the first organic light-emitting diode was invented with PN junction interface [6]. The typical materials for solar cells and transistors are Poly(3-alkylthiophenes). The (polyaniline, polyacetylene, and polypyrrole) are considered the main conductive polymers. Moreover, Poly(p-phenylenevinylene) (PPV) have appeared as the prototypical electroluminescent semiconducting polymers and used to produce the light, this device is called a polymer LED (Polymer Light-Emitting Diode, PLED). Now PPV has been considered as an extensive variety of applications due to its process ability, stability, and optical and electrical properties. The study of PLED / OLED is not only attracted by the researchers, but also involve in electronic industries. These industries have launched several kinds of multi-color full-color PLED / OLED display panel.

The organic semiconductor material used to produce many new optical components, such as solar cells, organic light emitting displays, organic thin film transistors (OTFT). Since the organic semiconductor material is more flexible and malleable than silicon, it can be formed on flexible plastic substrates. Organic flexible device which can be bend or twist, that opens a new way of low-cost plastic electronics. A lot of work has been done by the researcher on organic semiconductor materials and also this work is going ahead very rapidly specially on the charge-carrier density. Scientists are trying to find the new

materials able to achieve better and better performances. It is fact that organic electronics devices are able to compete inorganic electronics devices due to their easy production and mechanical flexibility.

Brédas et al. [7] demonstrated a theoretical characterization of charge transport organic π -conjugated polymers constitute the active elements in new generations of optoelectronic devices. Brédas and his coworkers shown in their work that charge transport in organic materials is extremely sensitive to the molecular packing, and arrangements can lead to electron mobilities are larger than hole mobilities. C. Tanase [8] concluded that hole-only diodes and FETs, with the same polymer act as an active material. Kelley and Muryes upgraded the carrier mobility of pentacene (pentacene) upto $5\text{cm}^2/\text{Vs}$ [9] which is more than the amorphous silicon carrier mobility. Garcia-Belmonte et al. [10] presented the behavioral consistency of P3HT and PCBM with a Schottky diode. They analyzed the charge carrier diffusion in ([6,6]-phenyl C61-butyric acid methyl ester (PCBM), and poly(3-hexylthiophene) (P3HT) with aluminum (Al) and indium tin oxide (ITO).

Lu Xiao and Sun [11] presented an extended Generalized Einstein relation (GER), they considered the potential energy of carriers in an electric field and concluded that the Generalized Einstein relation have position-dependent Fermi energy implies the organic semiconductor is in the electric field, and found out the ratio of diffusion coefficient to mobility. Blakesley et al. [12] studied the mobility of electrons and holes in two copolymers (fluorine based) at different temperatures with space-charge limited current measurements. They found out that the mobility was apparently dependent on the thickness of the polymer film. Oelerich et al suggested the determination of density of states in organic semiconductors related to the theory of concentration-dependent mobility, and proposed disordered organic semiconductors on the basis of previous theoretical DOS. When they compared the theoretical and experimental data they proved that the DOS (density of states) is not entirely an exponential function, which is differ than the present most of literature assumptions [13]. The mobility is strongly affected by the charge carrier concentration, and the conductivity depends only on the disorder of tail state whereas both mobility and conductivity are temperature dependence [14]. Different theories have been developed and many of models have been proposed for the carrier transport in organic semiconductor. Many theoretical DOS (Density of State) mobility transport models were proposed for the organic semiconductor with free carriers and trapped carriers [15-20]. It is pointed out that the mobility can be treated as independent to electric field by considering neutral condition as the applied voltage is zero, and the mobility can be treated as exponential function of root of electric field by ignoring the neutral condition [21].

In this work mobility behavior is analyzed in different organic polymers diodes at different temperatures by applying the mobility model using the theories like Drift Diffusion equation, Poisson's equation, Boltzmann

distribution law, Fermi Level. The transport mechanism of charge carriers is very important for synthesis of materials and enhance the performance of organic devices. All charge carrier transport mobility models have some shortcomings, so in this work improved analytic current-voltage formulae base charge transport model is used in this literature which covers a large number of organic polymers materials and the results of current-voltage formulae base charge transport model transport model are better than Gaussian trap model [22].

2. Method and calculation

2.1. Fundamental formula

The space charge limited (SCL) current is described by the Poisson equation for electric field potential ϕ is as follows [18, 21, 23-25].

$$\frac{d^2\phi}{dx^2} = -\frac{q}{\epsilon_r\epsilon_0}p(x) \quad (1)$$

with elementary charge (q), coordinate (x), density of holes (p); free-space permittivity (ϵ_0), the dielectric constant of the semiconductor (ϵ_r). The drift-diffusion equation for current density J is as follows:

$$\begin{aligned} J(x) &= -q\mu_p(x)p(x)\frac{\partial\phi}{\partial x} - kT\mu_p(x)\frac{\partial p(x)}{\partial x} \\ J(x) &= -q\mu_n(x)p(x)\frac{\partial\phi}{\partial x} - kT\mu_n(x)\frac{\partial p(x)}{\partial x} \end{aligned} \quad (2)$$

where the notation μ_p is the mobility and μ_n for holes, and electrons. Let L is the thickness of organic layer. W_{left} is the contact ($x = 0$) on left-side with low potential barrier, and W_{right} is the contact ($x = L$) on the right-side with high potential barrier. The difference ($W_{right} - W_{left}$) = V_{bi} is the built potential in devices. The boundary or edge conditions is used as $p(0) = N_f \exp(-W_{left}/kT)$, $p(L) = N_f \exp(-W_{right}/kT)$, and for electron is $n(0) = N_f \exp(-W_{left}/kT)$, $n(L) = N_f \exp(-W_{right}/kT)$; $\phi(0) = W_{left} + V$, $\phi(L) = W_{right}$; $V - V_{bi} = \phi(0) - \phi(L)$.

In order to derive an analytic solution, the analytic linear approximation for the Poisson equation (1) can be

$$\phi(x) = V + b + (V_{bi} - V)\left(\frac{x}{L}\right) \quad (3)$$

where V_{bi} is a built-in potential in the devices with asymmetric contacts, b is also known as band-bending parameter [26] is given as

$$b = \frac{kT}{q} \left[\ln \left(\frac{q^2 N_v L^2}{2KT\epsilon} \right) - 2 \right] \quad (4)$$

And the diffusion current is given by

$$J = \frac{q N_p \mu (V_{bi} - V) \left[\exp\left(\frac{qV}{kT}\right) - 1 \right]}{L \exp\left(\frac{qb}{kT}\right) \left[\exp\left(\frac{qV}{kT}\right) - \exp\left(\frac{qV_{bi}}{kT}\right) \right]} \quad (5)$$

The electric field evaluated from Eq. (3) is an independent to coordinate

$$F = \frac{-\partial\phi(x)}{\partial x} = \frac{(V - V_{bi})}{L} \quad (6)$$

So, the derived analytical expression for hole only mobility is

$$\mu_p(F) = \mu_p(0) \exp(\gamma\sqrt{F}) \quad (7)$$

$$\left. \begin{aligned} J_p &= \frac{q N_f \mu_p(0) (V - V_{bi}) \left[\exp\left(\frac{qV}{kT}\right) - 1 \right] \exp\left[\gamma\sqrt{(V - V_{bi})/L}\right]}{L \exp\left(\frac{qb}{kT}\right) \left[\exp\left(\frac{qV}{kT}\right) - \exp\left(\frac{qV_{bi}}{kT}\right) \right]} \\ J_n &= \frac{q N_f \mu_n(0) (V - V_{bi}) \left[\exp\left(\frac{qV}{kT}\right) - 1 \right] \exp\left[\gamma\sqrt{(V - V_{bi})/L}\right]}{L \exp\left(\frac{qb}{kT}\right) \left[\exp\left(\frac{qV}{kT}\right) - \exp\left(\frac{qV_{bi}}{kT}\right) \right]} \end{aligned} \right\} \quad (9)$$

From above set of equation we see that if the value of γ is taken as zero, the set of Eq. (9) becomes the old formula [23]. Moreover, the Gaussian model [18, 22, 28] for density of state has been recognized: $D(E) = (N_0/\sigma\sqrt{2\pi}) \exp[-(E - E_v)^2/2\sigma^2]$, with width σ , center energy E_v , and the total number of states N_0

Considering the non-degeneracy of organic semiconductors, the density of holes can be expressed as [18, 29-30], $p = N_f \exp\left[\frac{-q\phi(x)}{kT}\right]$, and density of electron can express as $n = N_f \exp\left[\frac{-q\phi(x)}{kT}\right]$, with evaluated integral for density of state can be

$$\left\{ \begin{aligned} N_f &= \int_{-\infty}^{\infty} D_f(E) \exp\left[\frac{(E - E_F)}{kT}\right] dE \\ N_f &= N_0 \exp\left[\frac{(E_v - E_F)}{kT}\right] \exp\left[\frac{\sigma^2}{2(kT)^2}\right] \end{aligned} \right\} \quad (10)$$

The coefficient $\mu_p(0)$ and $\mu_n(0)$ in Eq. (7) and Eq. (8) respectively denotes the zero-field mobility [31] and its thermally activated way can be expressed as

$$\mu_p(0) = \mu_0 \exp(-\Delta/k_B T) \quad (11)$$

$$\mu_n(0) = \mu_0 \exp(-\Delta/k_B T) \quad (12)$$

The linear dependency between γ and $1/T$, is expressed as following empirical relation

$$\gamma = B \left(\frac{1}{k_R T} - \frac{1}{k_R T_n} \right) \quad (13)$$

2.2. Application to materials and results

Set of Eq. (9) based modified charge transport model [27] apply to different polymers: poly{[N,N_-bis(2-octyldodecyl)-naphthalene-1,4,5,8-bis(dicarboximide)-2,6-diyl]-alt-5,5_-(2,2_-dithiophene)}[P(NDI2OD-T2), Polyera ActivInk(N2200)] hole only with thickness 140

And expression for electron only mobility is

$$\mu_n(F) = \mu_n(0) \exp(\gamma\sqrt{F}) \quad (8)$$

with parameters $\mu_p(0)$ $\mu_n(0)$ and γ , and the electric field F . If substituting Eq. (6) into Eq. (7), and then Eq. (6) into Eq. (8), the mobility is independent to coordinate. Proceeding the above equations then the analytic JV formula for hole [23, 27] and for electron to following form

nm [32-33], poly{[N,N_-bis(2-octyldodecyl)-naphthalene-1,4,5,8-bis(dicarboximide)-2,6-diyl]-alt-5,5_-(2,2_-dithiophene)}[P(NDI2OD-T2), Polyera ActivInk(N2200)] electron only with thickness 360 nm [1,32-33], poly{[N,N_-bis(2-octyldodecyl)-naphthalene-1,4,5,8-bis(dicarboximide)-2,6-diyl]-alt-5,5_-(2,2_-dithiophene)}[P(NDI2OD-T2), Polyera ActivInk(N2200)] electron only with barium cathode with thickness 460 nm[15], poly[2,6-(4,4-bis(2-ethylhexyl)-4H-cyclopenta[2,1-b;3,4-b0]-dithiophene)-alt-4,7-(2,1,3-benzothiadiazole)]PCPDTBT 148 nm electron only diodes [22], (poly[2-methoxy-5-(30,70-dimethyloctyloxy)-p-phenylene vinylene] (OC₁₀-PPV) 300 nm electron-only diodes [22].

J-V curves is calculated from analytic Eq. (9) and numerical solutions of Eqs.(1, 2). The theoretical results (plotted JV curves) are compared with experimental points (square points) in Figs. 1-5.

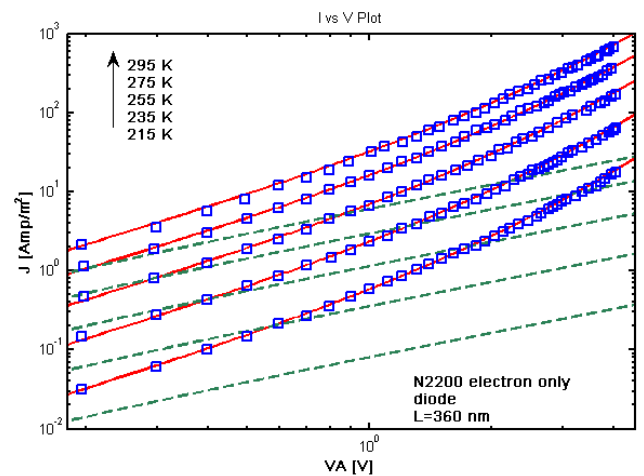


Fig. 1. Balancing of calculated J-V curves by using modified model with experimental data (square symbols) for N2200 electron only diode with thickness of organic layer $L=360$ nm at different temperatures. (solid lines indicate when $\gamma \neq 0$ (modified transport model); dashed lines indicate when $\gamma = 0$) (color online)

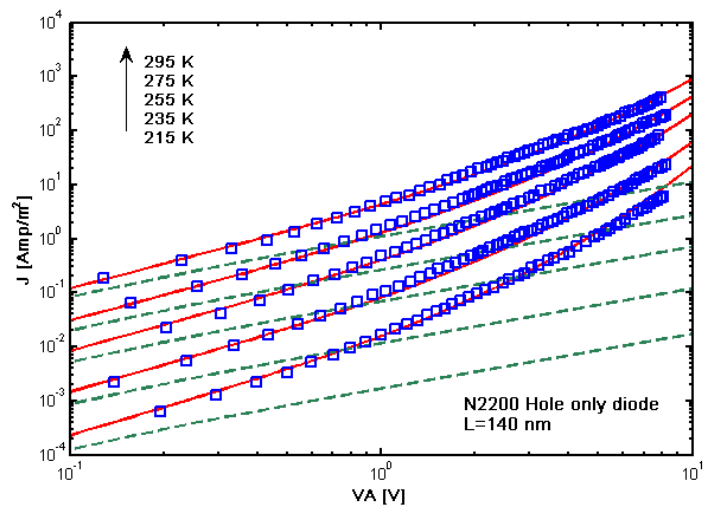


Fig. 2. Balancing of calculated J - V curves by using modified model with experimental data for N2200 hole only diode with thickness of organic layer $L=140$ nm at different temperatures. (solid lines indicate when $\gamma \neq 0$ (modified transport model); dashed lines indicate when $\gamma = 0$) (color online)

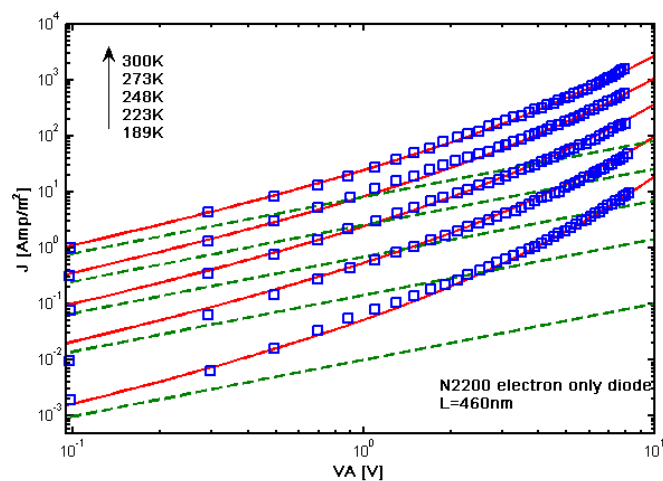


Fig. 3. Balancing of calculated J - V curves by using modified model with experimental data for N2200 electron only diode with barium cathode with thickness of organic layer $L=460$ nm at different temperatures. (solid lines indicate when $\gamma \neq 0$ (modified transport model); dashed lines indicate when $\gamma = 0$) (color online)

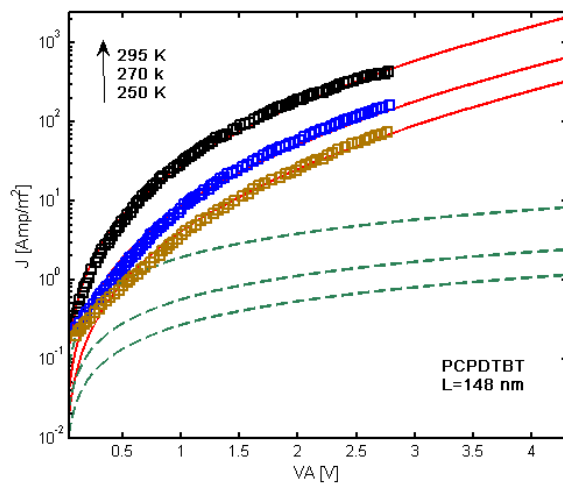


Fig. 4. Balancing of calculated J - V curves by using modified model with experimental data for PCPDTBT with thickness of organic layer $L=148$ nm at different temperatures. (solid lines indicate when $\gamma \neq 0$ (modified transport model); dashed lines indicate when $\gamma = 0$) (color online)

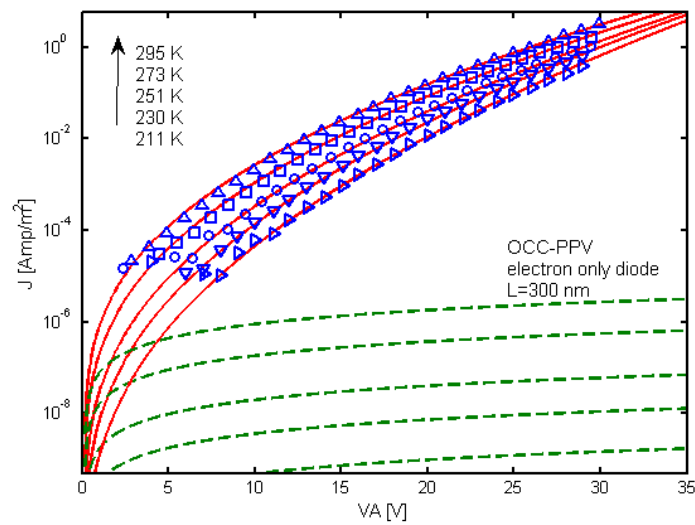


Fig. 5. Balancing of calculated J-V curves by using modified model with experimental data for OC₁C₁₀-PPV electron only diode with thickness of organic layer $L=300$ nm at different temperatures. (solid lines indicate when $\gamma \neq 0$ (modified transport model); dashed lines indicate when $\gamma = 0$) (color online)

These plotted figures depict an excellent agreement between theoretical curves (solid lines) with experimental data (square points) which covers all voltages range and temperatures. In Figs.1-5 there is no contrast between results of Eq. (9) and the numerical solutions of Eqs. (1, 2). So, the modified formula in Eq. (9) is a best approximation to numerical solutions of Eqs. (1, 2). Specially the results show in Figs. 4 and 5 is far better than the [22]. In Figs.1-5 we see the importance of γ when the

value of γ is taken as zero the results (dotted lines) diverge from the experiment data (square points) and fittings of J-V data at high and low voltage is not good.

The significant analyses of the variations of fitting N_f with temperature is also calculated by using Eq. (10). The fitted curves are compared with optimized points in Figs. 6-9 respectively.

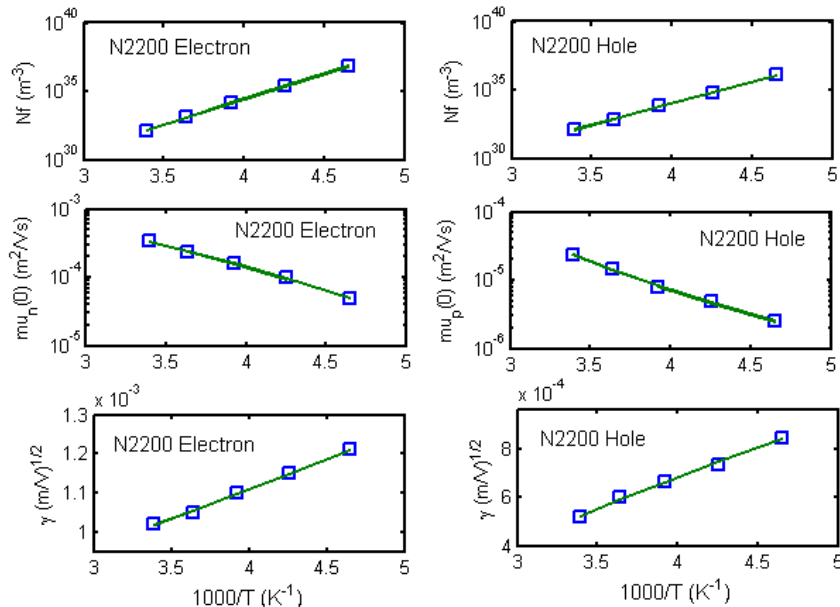


Fig. 6. Variations of $N_f(T)$, $\mu_p(0)$, $\mu_n(0)$, and $\gamma(T)$ for N2200 electron only ($L=360$ nm) and hole only ($L=140$ nm) diode with respect to temperature smoothed by using Eqs. (10-13) (color online)

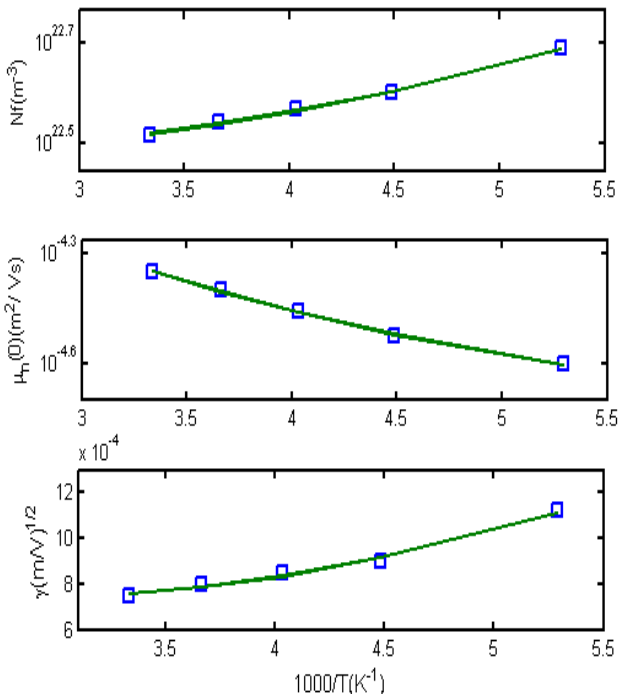


Fig. 7. Variations of $N_f(T)$, $\mu_n(0)$, and $\gamma(T)$ for N2200 electron only ($L=460$ nm) diode with respect to temperature smoothed by Eq. (10), Eq.(12), and Eq. (13) (color online)

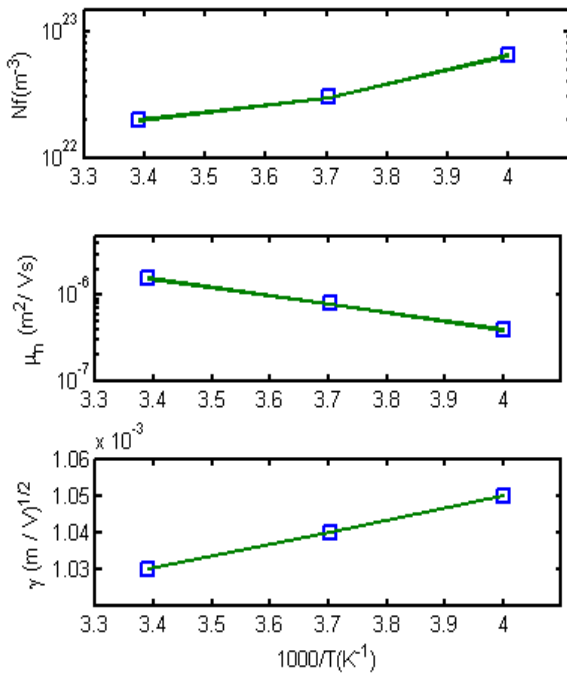


Fig. 8. Variations of $N_f(T)$, $\mu_n(0)$, and $\gamma(T)$ for PCPDTBT with 148 nm thickness diode with respect to temperature smoothed by using Eq. (10), Eq.(12), and Eq. (13) (color online)

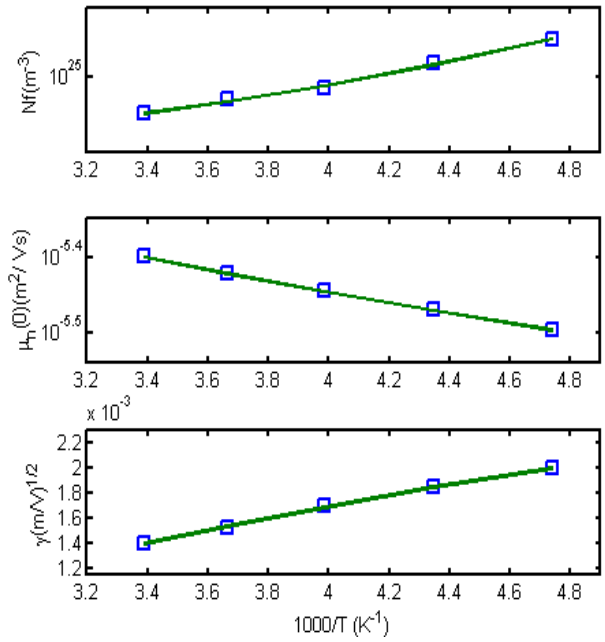


Fig. 9. Variations of $N_f(T)$, $\mu_n(0)$, and $\gamma(T)$ for OCC-PPV electron only diode with 300 nm thickness diode with respect to temperature smoothed by using Eq. (10), Eq.(12), and Eq. (13) (color online)

Figs. 6-9 also depict the variations of parameters μ_p / μ_n and γ with temperature. In these figures, we also plot curves smoothed by using Eq. (11) / Eq. (12) and Eq. (13). The respective figures show that μ_p / μ_n can be well fitted by using Eq. (11) / Eq. (12). The variation of μ_p / μ_n with temperature well obeys the Arrhenius relationship in Eq. (11) / Eq. (12). These figures also show that γ can be well fitted by using Eq. (13), the smoothed curves are in good agreement with experimental points.

Table 1 shows the value of potential barriers for following materials. The values of W_{right} are always greater than the value of W_{left} , which shows the asymmetric positive built potential. Moreover the plotted variation of parameters $\mu_p(0)$, $\mu_n(0)$, and γ with temperature, and curves smoothed by using Eqs. (11, 12, 13) as shown in their respective Figs. 6-9. These figures show that Eqs. (11, 12, 13) is well fitted with the data points.

Table 1. W_{left} (eV) and W_{right} (eV) optimized by fitting J-V data for N2200 electron only L=360 nm, N2200 hole only L=140 nm, N2200 electron only L=460 nm, PCPDTBT electron only L=148 nm, OCC-PPV electron only L=300 nm organic diodes

| Potential | N2200 (electron only) (360 nm) | N2200 (hole only) (140 nm) | N2200 (electron only) (460 nm) | PCPDTBT (electron) (148 nm) | OCC-PPV (electron only) (300 nm) |
|------------------|--------------------------------------|----------------------------------|--------------------------------------|-----------------------------------|--|
| W_{left} (eV) | 0.91 | 0.91 | 0.286 | 0.249 | 0.78 |
| W_{right} (eV) | 0.94 | 0.94 | 0.288 | 0.253 | 0.94 |

So, the analytic J-V formulae in Eq. (9) with expressions for parameters in Eqs. (11, 12, 13) are simple and sound tool for organic diodes. The quality of fitted smoothed values of N_f , $\mu(0)$ and γ is fine and satisfactory. The values of temperature dependent parameter N_f , $\mu_n(0)$,

$\mu_p(0)$, γ are listed in Table 2, which indicate the appropriation that the mobility is the increasing function of temperature.

Table 2. Temperature-dependent parameters N_f , μ_n , μ_p , and γ optimized by fitting J-V data for N2200 electron only L=360 nm, N2200 hole only L=140 nm, N2200 electron only L=460 nm, PCPDTBT electron only L=148 nm, OCC-PPV electron only L=300 nm organic diodes

| | | | | | | |
|---|---------------------------------|------------|------------|------------|------------|------------|
| N2200 (electron only) (360 nm) | T (K) | 215 | 235 | 255 | 275 | 295 |
| | N_f (m ⁻³) | 8E36 | 2.7E35 | 1.6E34 | 1.35E33 | 1.45E32 |
| | $\mu_n(0)$ (m ² /Vs) | 0.5E-4 | 1E-4 | 1.6E-4 | 2.4E-4 | 3.4E-4 |
| | γ (m/V) ^{1/2} | 0.00121 | 0.00115 | 0.00110 | 0.00105 | 0.00102 |
| N2200 (hole only) (140 nm) | T (K) | 215 | 235 | 255 | 275 | 295 |
| | N_f (m ⁻³) | 1.3E36 | 7E34 | 7.5E33 | 7.65E32 | 1.45E32 |
| | $\mu_p(0)$ (m ² /Vs) | 2.5E-6 | 4.9E-6 | 8E-6 | 1.48E-5 | 2.4E-5 |
| | γ (m/V) ^{1/2} | 0.00085 | 0.00074 | 0.00067 | 0.0006 | 0.00052 |
| N2200(electron only) (460 nm) | T (K) | 189 | 223 | 248 | 273 | 300 |
| | N_f (m ⁻³) | 4.9E22 | 4E22 | 3.7E22 | 3.5E22 | 3.3E22 |
| | $\mu_n(0)$ (m ² /Vs) | 2.5E-5 | 3E-5 | 3.5E-5 | 4E-5 | 4.5E-5 |
| | γ (m/V) ^{1/2} | 0.00112 | 0.0009 | 0.00085 | 0.00080 | 0.00075 |
| PCPDTBT (electron only) (L=148 nm) | T (K) | 250 | 270 | 295 | | |
| | N_f (m ⁻³) | 4E22 | 3E22 | 2E22 | | |
| | $\mu_n(0)$ (m ² /Vs) | 6.5E-7 | 8E-7 | 1.6E-6 | | |
| | γ (m/V) ^{1/2} | 0.00105 | 0.00104 | 0.00103 | | |
| OCC-PPV (electron only) (300 nm) | T (K) | 211 | 230 | 251 | 273 | 295 |
| | N_f (m ⁻³) | 1.22E26 | 2.5E25 | 4.8E24 | 2.3E24 | 9.0E23 |
| | $\mu_n(0)$ (m ² /Vs) | 3.2E-6 | 3.4E-6 | 3.6E-6 | 3.8E-6 | 4E-6 |
| | γ (m/V) ^{1/2} | 0.002 | 0.00184 | 0.00170 | 0.00152 | 0.00140 |

Furthermore apply modified formula based model in Eq. (9) to polyalkoxyspirobifluorene-N,N,N',N'-tetraaryldiamino biphenyl (PSF-TAD) copolymer with

different layer thicknesses at 295K[34], poly(fluorene-triarylamine) and polymer hole only device with different layer thicknesses at room temperature [35].

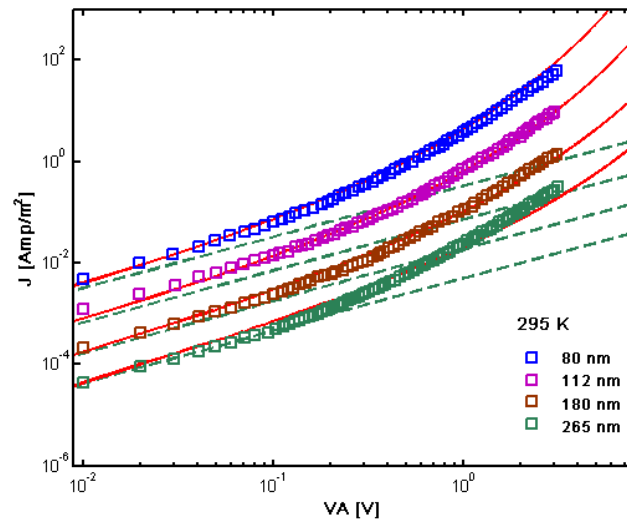


Fig. 10. Balancing of calculated J-V curves by using modified model with experimental data for polyalkoxyspirobifluorene-*N,N,N',N'*-tetraaryldiamino biphenyl (PSF-TAD) copolymer different layer thicknesses at 295K (solid lines indicate when $\gamma \neq 0$ (modified transport model); dashed lines indicate when $\gamma = 0$) (color online)

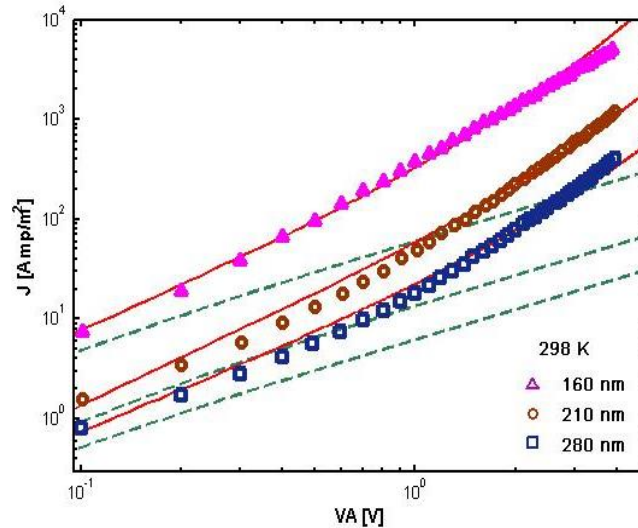


Fig. 11. Balancing of calculated J-V curves by using modified model with experimental data for hole-only J(V) curves for polymer Hole only device for polymer films copolymer different layer thicknesses at 298K (solid lines indicate when $\gamma \neq 0$ (modified transport model); dashed lines indicate when $\gamma = 0$) (color online)

J-V curves are calculated from analytic Eq. (9) and numerical solutions of Eqs. (1,2) for above two materials. The theoretical results (plotted JV curves) are compared with experimental points (square points) in Figs. 10, 11. These figures show the excellent agreement between theoretical curves (solid lines) with experimental data (square points).

The dotted deviated line indicates when the value of γ is taken as zero which is not agree with the experiment

data (square points). Hence the modified formula is the best approximation to the numerical solutions. In Tables 3, and 4 all parameters of (PSF-TAD), and hole only device with different thickness is listed. Tables 3, and 4 show that the value of $\mu_p(0)$, γ , N_f is same for each material with different thicknesses. The values of W_{right} and W_{left} , is also listed in Tables 3, 4, and 5. The values of W_{right} are always greater than the value of W_{left} , which shows the asymmetric positive built potential.

Table 3. Parameters with constant value N_f , μ_n , and γ of polyalkoxyspirobifluorene-*N,N,N',N'*-tetraaryldiamino biphenyl (PSF-TAD) copolymer different layer thicknesses at 295 K

| T (K) | Thickness (nm) | $\mu_p(0)$ (m^2/Vs) | $\gamma(m/V)^{1/2}$ | N_f (m^{-3}) | W_{right} (eV) | W_{left} (eV) |
|-------|----------------|-------------------------|---------------------|--------------------|------------------|-----------------|
| 295 | 80 | 1.8E-12 | 0.00073 | 8.28E25 | 0.175 | 0.173 |
| 295 | 112 | 1.8E-12 | 0.00073 | 8.28E25 | 0.207 | 0.203 |
| 295 | 180 | 1.8E-12 | 0.00073 | 8.28E25 | 0.233 | 0.225 |
| 295 | 265 | 1.8E-12 | 0.00073 | 8.28E25 | 0.258 | 0.249 |

Table 4. Parameters with constant value N_f , μ_n , and γ of polymer hole only device with different layer thicknesses at room temperature

| $T(K)$ | Thickness (nm) | $\mu_p(0)$ (m^2/Vs) | $\gamma(m/V)^{1/2}$ | $N_f(m^{-3})$ | W_{right} (eV) | W_{left} (eV) |
|--------|----------------|-------------------------|---------------------|---------------|------------------|-----------------|
| 298 | 160 | 3.5E-5 | 0.00069 | 2.25E30 | 0.74 | 0.716 |
| 298 | 210 | 3.5E-5 | 0.00069 | 2.25E30 | 0.785 | 0.747 |
| 298 | 280 | 3.5E-5 | 0.00069 | 2.25E30 | 0.78 | 0.76 |

3. Conclusion

In this paper, the modified J-V formula-based charge transport model is applied to several hole only, and electron only devices of various thicknesses at different temperatures. It is verified that results obtained from the modified charge transport model arrived at a good agreement with the experimental data points as compared to original transport model. In this paper it is also analyzed that the modified J-V formula-based charge transport model support the quantum chemical study for material such as Poly{[N,N'-bis(2-octyldodecyl)-naphthalene-1,4,5,8-bis(dicarboximide)-2,6-diyl]-alt-5,5'-(2,2'-dithiophene)}[P(NDI2ODT2),PolyeraActivInk™(N2200)] in which the electron mobility is observed to be more than the hole mobility. This work confirms that the improved formula-based charge transport model is more precise and convenient for applications, and covers a large number of materials and helps to modify the semiconductor devices in more precise form with better performance.

References

- [1] Sebastian Reineke, Frank Lindner, Gregor Schwartz, Nico Seidler, Karsten Walzer, Björn Lüssem, Karl Leo, *Nature* **459**, 234 (2009).
- [2] V. Coropceanu, J. Cornil, D. A. da Silva Filho, Y. Olivier, R. Silbey, J. L. Brédas, *Chemical reviews* **107**(4), 926 (2007).
- [3] K. Pei, *Surfaces and Interfaces* **30**, 101887 (2022).
- [4] M. A. Khan, A. N. Khan, A. S. Zalhaf, *Sciencetech.* **2**(2), 18 (2021).
- [5] M. H. Gharahcheshmeh, K. K. Gleason, *Energies* **15**(10), 3661 (2022).
- [6] C. W. Tang, S. A. Vanslyke, *Applied Physics Letters* **51**(12), 913 (1987).
- [7] J. L. Brédas, J. P. Calbert, D. A. Da Silva Filho, J. Cornil, *Proceedings of the National Academy of Sciences* **99**(9), 5804 (2002).
- [8] C. Tanase, E. J. Meijer, P. W. M. Blom, D. M. de Leeuw, *Physical Review Letters* **91**(21), 216601 (2003).
- [9] T. W. Kelley, D. V. Muires, F. P. Baude, T. P. Smith, T. D. Jones, *Materials Research Society Symposium- Proceedings*, **771**, L6-5 (2003).
- [10] G. Garcia-Belmonte, A. Munar, E. M. Barea, J. Bisquert, I. Ugarte, R. Pacios, *Organic Electronics* **9**(5), 847 (2008).
- [11] X. H. Lu, J. X. Sun, Y. Guo, D. Zhang, *Chinese Physics Letters* **26**(8), 087202 (2009).
- [12] J. C. Blakesley, H. S. Clubb, N. C. Greenham, *Physical Review B* **81**(4), 045210 (2010).
- [13] J. O. Oelerich, D. Hueimmer, S. D. Baranovskii, *Physical Review Letters* **108**(22), 226403 (2012).
- [14] L. Jun, S. Jiu-Xun, C. Zhao, *Synthetic Metals* **159**(19-20), 1915 (2009).
- [15] R. Steyrleuthner M. Schubert, F. Jaiser, J. C. Blakesley, Z. Chen, A. Facchetti, D. Neher, *Advanced Materials* **22**(25), 2799 (2010).
- [16] Y. Hu, J. Yin, X.H. Ju, *J. Optoelectron. Adv. M.* **17**(9-10), 1556 (2015).
- [17] A. Y. Sosorev, *Materials and Design*, **192**, 108730 (2020).
- [18] M. A. Khan, S. Jiu-Xun, J. Ke, C. Ling-Cang, W. Qiang, *RSC Advances* **5**(5), 3113 (2015).
- [19] L. G. Wang, Y. X. Gao, X. L. Liu, L. F. Cheng, *J. Optoelectron. Adv. M.* **18**(5-6), 504 (2016).
- [20] Y. F. Li, Y. J. Wang, L. G. Wang, Y. Guo, L. Zhang, *J. Optoelectron. Adv. M.* **24**(3-4), 146 (2022).
- [21] M. A. Khan, J. X. Sun, *Chinese Physics B* **24**(4), 047203 (2015).
- [22] H. T. Nicolai, M. Kuik, G. A. H. Wetzelaer, B. de Boer, C. Campbell, C. Risko, J. L. Brédas, P. W. M. Blom, *Nature Materials* **11**(10), 882 (2012).
- [23] P. de Bruyn, A. H. P. van Rest, G. A. H. Wetzelaer, D. M. de Leeuw, P. W. M. Blom, *Physical Review Letters* **111**(18), 186801 (2013).
- [24] A. Salleo, T. W. Chen, A. R. Völkel, Y. Wu, P. Liu, B. S. Ong, R. A. Street, *Physical Review B* **70**(11), 115311 (2004).
- [25] S. V. Yampolskii, Y. A. Genenko, C. Melzer, H. von Seggern, *Journal of Applied Physics* **109**(7), 073722 (2011).
- [26] J. G. Simmons, *Journal of Physics and Chemistry of Solids* **32**(8), 1987 (1971).
- [27] M. A. Khan, S. Jiu-Xun, *RSC Advances* **5**(24), 18720 (2015).
- [28] C.-X. Zhou, J.-X. Sun, Z.-J. Deng, S. Zhou, *Semiconductors* **47**, 1351 (2013).
- [29] W. F. Pasveer, J. Cottaar, C. Tanase, R. Coehoorn, P. A. Bobbert, P. W. M. Blom, D. M. De Leeuw, M. A. J. Michels, *Physical Review Letters* **94**(20), 206601 (2005).
- [30] S. L. M. Van Mensfoort, R. Coehoorn, *Physical Review B* **78**(8), 085207 (2008).
- [31] S. Züfle, S. Altazin, A. Hofmann, L. Jäger, M. T. Neukom, W. Brütting, B. Ruhstaller, *Journal of Applied Physics* **122**(11), 115502 (2017).
- [32] G. J. A. H. Wetzelaer, M. Kuik, Y. Olivier, V. Lemaire, J. Cornil, S. Fabiano, M. A. Loi, P. W. Blom, *Physical Review B* **86**(16), 165203 (2012).
- [33] Z. Chen, Y. Zheng, H. Yan, A. Facchetti, *Journal of*

- the American Chemical Society **131**(1), 8 (2009).
- [34] G. A. H. Wetzelaer, P. W. M. Blom, Physical Review **B 89**(24), 241201 (2014).
- [35] M. A. Muth, W. Mitchell, S. Tierney, T. A. Lada, X. Xue, H. Richter, M. Carrasco-Orozco, M. Thelakkat, Nanotechnology **24**(48), 484001 (2013).

*Corresponding author: ammar@qurtuba.edu.pk